Inorganic Chemistry

Article

pubs.acs.org/IC

Heptabismuthate $[Bi_7I_{24}]^{3-}$: A Main Group Element Anderson-Type Structure and Its Relationships with the Polyoxometalates§

Kirill Yu. Monakhov,† Christophe Gourlaouen,‡ Roberto Pattacini,† and Pierre Braunstein*,†

†Laboratoire de Chimie de Coordination and ‡Laboratoire de Chimie Quantique, Institut de Chimie (UMR 7177 CNRS), Université de Strasbourg, 4 rue Blaise Pascal, CS 90032, F-67081 Strasbourg Cedex, France

Supporting Information

ABSTRACT: We describe the unique structural and electronic arrangement in the heptanuclear polyiodobismuthate $[Bi_7I_{24}]^{3-}$ which displays striking similarities with the Anderson-type structures found in polyoxometalates. This main group element anion is part of the complex $[Bi(OAc)_2(thf)_4]_3[Bi_7I_{24}]$ (**1**) which has been characterized by X-ray crystallography. We investigated the structure, stability, and bonding of $[Bi_7I_{24}]^{3-}$ using relativistic dispersion-corrected density functional theory in combination with a quantitative energy decomposition and electron localization function analysis in order to better understand the main features of this isopolyanion. A comparative analysis of the properties of $[Bi_7I_{24}]^{3-}$ and previously reported high-nuclearity $[Bi_nX_{3n+m}]^{m-}$ anions, in the gas phase and in solution, has been performed, in the latter case to track the macroscopic solvent effects. $[Bi_7I_{24}]^{3-}$ is the largest building block in the class of trianionic iodobismuthates and the sole heptanuclear framework in the family of iodobismuthates.

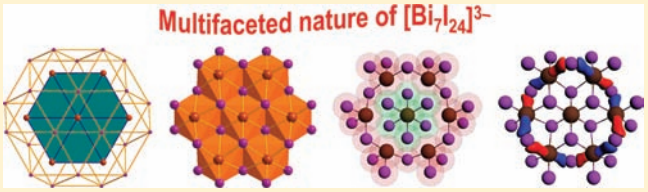

INTRODUCTION

Establishing structural relationships between main group and transition metal compounds allows one to create fruitful bridges between seemingly different chemistries, and this has generated increasing interest, in particular since the development of the isolobal analogy concept.[1] Whether structural analogies between metal complexes translate into similar electronic structures remains a fascinating research topic, not least because of the considerable structural and bonding diversity encountered in inorganic chemistry.[2]

The structural chemistry of highly aggregated alkali metal salts of "elementanediides" $[RE]^{2-}$ (E = P, As, Bi),[3] which are unique multiple-shell compounds and excellent container molecules, can easily be compared with that of the polyoxometalates (POMs) with Lindqvist-, α-Keggin-, or Wells–Dawson-type frameworks, which are much investigated owing to their rich chemical and physical properties.[4,5] In particular, the structures of some polynuclear bismuth compounds display striking similarities with those of POMs.[3c,d]

Iodobismuthates have fascinating optical, electrical, electronic, and magnetic properties,[6] and their versatile structural chemistry is of high current interest.[7] To date, the structures available for the binary complexes $[Bi_xI_y]^{m-}$ $(m = y - 3x)$[7] include the following: mononuclear BiI_3, $[BiI_4]^-$, $[BiI_5]^{2-}$, and $[BiI_6]^{3-}$; dinuclear Bi_2I_6, $[Bi_2I_8]^{2-}$, $[Bi_2I_9]^{3-}$, and $[Bi_2I_{10}]^{4-}$; trinuclear $[Bi_3I_{11}]^{2-}$ and $[Bi_3I_{12}]^{3-}$; tetranuclear $[Bi_4I_{14}]^{2-}$ and $[Bi_4I_{16}]^{4-}$; pentanuclear $[Bi_5I_{18}]^{3-}$ and $[Bi_5I_{19}]^{4-}$; hexanuclear $[Bi_6I_{22}]^{4-}$; and octanuclear $[Bi_8I_{28}]^{4-}$ and $[Bi_8I_{30}]^{6-}$. Many of those complexes were prepared in situ under rather severe conditions (high-temperature and/or solvothermal reactions). Herein, we report the structural and computational studies of the first heptanuclear complex in this series, $[Bi_7I_{24}]^{3-}$, obtained under very mild conditions. It is noteworthy that $[Bi_7I_{24}]^{3-}$ has been briefly mentioned previously;[8] however, no detailed synthesis or structural data were available. We shall see below that the framework of $[Bi_7I_{24}]^{3-}$ is of great interest, in particular, because it possesses an Anderson-type structure which is remarkably similar to that of hetero- and isopolyoxoanions $[XM_6O_{24}]^{6-}$ (X = Te; M = Mo, W).[5a,b] For this reason, use of theoretical approaches to better understand and rationalize the structure and composition of this heptanuclear iodobismuthate trianion and its lighter homologues was felt highly desirable.

RESULTS AND DISCUSSION

With the initial aim to form mixed Bi–Pd complexes, we reacted a 2-fold excess of BiI_3 with $[Pd(OAc)_2]$ in tetrahydrofurane (thf) under ambient conditions and obtained the highly associated salt $[Bi(OAc)_2(thf)_4]_3[Bi_7I_{24}]$ (**1**) as the result of a ligand-exchange reaction (Supporting Information). The reaction does not take place in the presence of noncoordinating solvents, e.g., CH_2Cl_2, because a donor solvent is crucial in stabilizing the countercation associated with $[Bi_7I_{24}]^{3-}$.

Compound **1** crystallizes with four H_2O molecules in the trigonal space group $R\bar{3}c$ (Figure 1, Table S2 and Figure S2, Supporting Information).[9] Similarly to the behavior of $[Na_3(thf)_x]_3[Bi_7I_{24}]$,[8] red crystalline **1**·4H_2O is extremely sensitive to loss of the thf molecules from its cation (Figure S1, Supporting Information).

Received: August 25, 2011
Published: January 9, 2012

   dx.doi.org/10.1021/ic201859c | *Inorg. Chem.* 2012, 51, 1562–1568

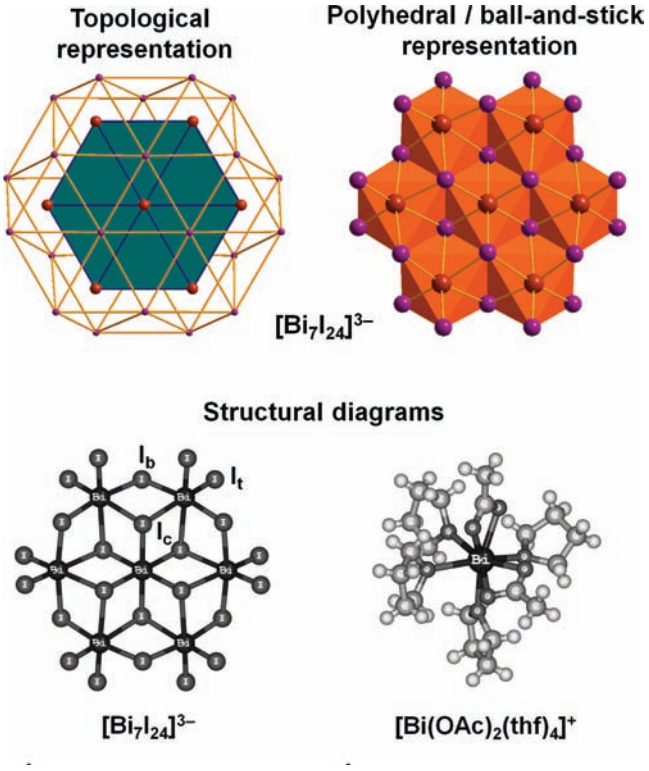

Figure 1. (Top) $[Bi_7I_{24}]^{3-}$ in topological (as $[Bi_7@(I_{24})]^{3-}$) and polyhedral/ball-and-stick (Anderson-type) representations. Color code: Bi, maroon; I, violet. (Bottom) Structural diagrams of molecular units **1b** (left) and **1a** (right) in the crystal of $\mathbf{1}\cdot 4H_2O$.

In the $[Bi(OAc\text{-}\kappa^2O)_2(thf)_4]^+$ cation (**1a**) the bismuth center is octacoordinated (Figure 1) with two chelating acetate groups and four thf molecules which interact with bismuth via ion–dipole Bi···O contacts. Unfortunately, a discussion of the bond lengths and angles is not possible owing to the uncertainties associated with refinement of the lighter atoms (Supporting Information).

The structure of the trianion $[Bi_7I_{24}]^{3-}$ (**1b**) displays a noncrystallographic S_6 symmetry and is of the Anderson type, with six edge-sharing BiI_6 octahedral moieties arranged in a cyclic manner ($Bi_6(\mu_2\text{-}I_b)_6$ ring) through six Bi–(μ_2-I_b)–Bi bridges connected to the central BiI_6 octahedron through six μ_3-I_c ligands. The remaining 12 iodine atoms (I_t) are terminally bound and coordinated to the bismuth atoms which form the $Bi_6(\mu_2\text{-}I_b)_6$ ring. These I_t atoms form in the solid-state intermolecular $I_t\cdots I_t$ contacts in the range of 362.1(2)–366.2(3) pm with the neighboring $[Bi_7I_{24}]^{3-}$ units (Figure 2). These values are smaller than the sum of the iodine van der Waals radii ($\Delta\Sigma r_{vdW}$ = 420[10a] and 396 pm[10c]).[10] We note, of course, that the general structural pattern of **1b** based on interlinked BiI_6 octahedra is well established for other known iodobismuthates with extended structures.[7]

In order to rationalize the structure of $[Bi_7I_{24}]^{3-}$ and explore its relationship with that of Anderson-type POMs, a computational study was undertaken and two models were considered, A and B (Figure 3). Model A describes the interactions between a negatively charge unit (or "guest") and a hypothetical neutral $[Bi_6I_{18}]$ crown (as "receptor") containing a planar Bi_6 ring. This model is related to that elaborated for the Anderson-type POMs $[TeM_6O_{24}]^{6-}$ (M = Mo, W).[5a,b] Model B describes the interaction between a central Bi^{3+} cation and a hypothetical ionic crown $[Bi_6I_{24}]^{6-}$. This model is reminiscent of the structures recently found in new open-shell Anderson-type nickel and cobalt polyoxocations of the type $[XM_6O_{12}L_{12}]^+$ (X = Na^+; M = Ni^{2+}, Co^{2+}; L = (pyridine-2-yl)methanolate).[11]

Geometry optimization of $[Bi_7I_{24}]^{3-}$ with an overall D_{3d} symmetry was first carried out without and then with inclusion of the London dispersion effects in the gas phase (see Figure S3, Supporting Information). In model A, the assembling of the octahedral $[BiI_6]^{3-}$ with the $[Bi_6I_{18}]$ unit of D_{6h} point group symmetry to form **I** results in ca. 10% expansion of the planar Bi_6 ring in $[Bi_7I_{24}]^{3-}$ (Figures 3 and S3, Supporting Information). In contrast, model B results in ca. 2% contraction of the Bi_6 ring on going from the D_{3d} symmetrical $[Bi_6I_{24}]^{6-}$ to **II**, owing to encapsulation of a Bi^{3+} ion (Figures 3 and S3, Supporting Information). The Bi···Bi distances found for $[Bi_7I_{24}]^{3-}$ in the crystal structure of $\mathbf{1}\cdot 4H_2O$ are ca. 5% shorter than those obtained by DFT (Figure S3, Supporting Information). The experimental value of $d_{Bi\cdots Bi}$ = 469.2 pm ($\mathbf{1}\cdot 4H_2O$; see the Supporting Information for a list of the Bi···Bi distances with standard deviations) is either shorter than the sum of the bismuth van der Waals radii $\Delta\Sigma r_{vdW}$ = 480 pm[10a] or

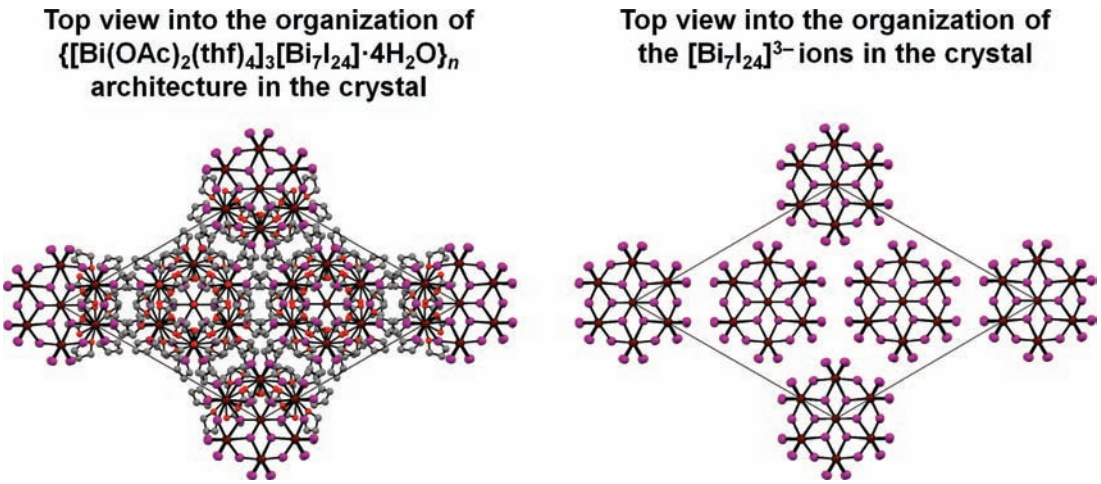

Figure 2. Structural diagrams of the solid-state structure of $\mathbf{1}\cdot 4H_2O$ (left) and without the cations (right). Color code: Bi, maroon; I, violet; O, red; C, gray. Hydrogen atoms are omitted for clarity.

dx.doi.org/10.1021/ic201859c | Inorg. Chem. 2012, 51, 1562–1568

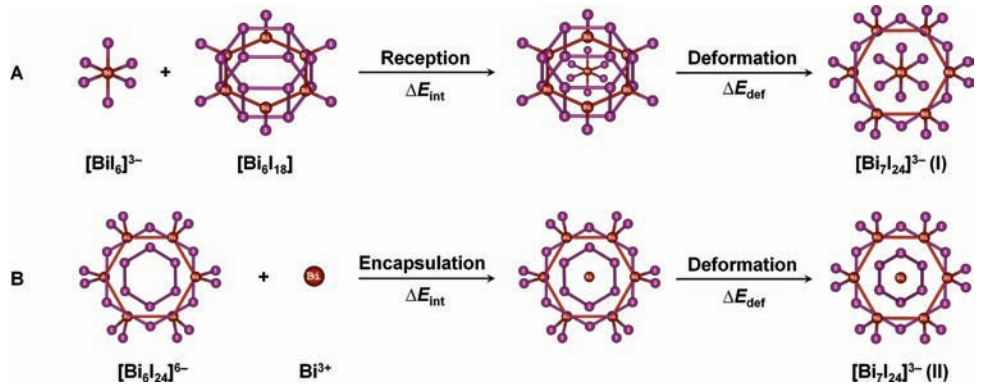

Figure 3. Topological representations of the theoretically analyzed association processes between (A) the $[BiI_6]^{3-}$ unit and the $[Bi_6I_{18}]$ crown (top) and (B) the $[Bi_6I_{24}]^{6-}$ crown and the cation Bi^{3+} (bottom) which result in $[Bi_7I_{24}]^{3-}$, represented as **I** and **II**, respectively. The top model (A) describes the process where the octahedral unit $[BiI_6]^{3-}$ interacts with the hexagonal $Bi_6(I_t)_6$ subunit inscribed in a cyclic hexagonal prismatic I_{12} subshell. The bottom model (B) describes the process where Bi^{3+} occupies the center of a hexagonal I_6 unit of the $[Bi_6I_{24}]^{6-}$ crown.

longer if the value of $\Delta\Sigma r_{vdW}$ = 414 pm[10c] is considered. The BP86-optimized distance of 493.6 pm for the Bi···Bi separations is ca. 5% longer than the experimental one. The experimental $Bi_{crown}-I_t$, $Bi_{crown}-I_b$, $Bi_{crown}-I_c$, and $Bi_{center}-I_c$ bond lengths are 1−3% shorter than those obtained by relativistic DFT (Figure S3, Supporting Information). This originates from use of the dispersion-noncorrected BP86 functional which leads one to underestimate the instantaneous dipole-induced forces in the trianion and results in relaxation of the gas-phase structure of $[Bi_7I_{24}]^{3-}$. Inclusion of the effects of long-range van der Waals interactions (dispersion terms[12,13]) in the geometry optimizations reduces all bond lengths in $[Bi_7I_{24}]^{3-}$ and its constitutive fragments (Figure S3, Supporting Information) and also lowers the total bonding energy. This was verified using the first and third generations of Grimme's dispersion correction (DFT-D and DFT-D3, respectively).[12] Thus, the contribution of the intramolecular dispersion energy, ΔE_{disp}, in $[Bi_7I_{24}]^{3-}$ is about 1.3 times larger than that for the anionic cage $[Bi_6I_{24}]^{6-}$, 1.8 times larger than for the neutral cage $[Bi_6I_{18}]$, and 10 times larger than for the parent $[BiI_6]^{3-}$ unit (Table S3, Supporting Information). As a result, the equilibrium structure of $[Bi_7I_{24}]^{3-}$ optimized in the gas phase at the BP86-D level of theory is in excellent agreement with the experimental solid-state structure of this trianion in $\mathbf{1}\cdot 4H_2O$. The adequacy of the calculation model was also shown by the only minor difference of ca. −7 kcal mol^{-1} between the total energies of the optimized and experimental structures.

To explore the origin of the dispersion effects encountered, electron localization function (ELF) analyses were performed on the BP86(-D)-optimized structures of **I** and its fragments according to model A. A whole set of bismuth valence basins are present on the isolated $[Bi_6I_{18}]$ crown (Figure 4). Similar metallic valence basins have been observed in asymmetric complexes of Pb(II) ($[Hg]6p^0$), which has the same electronic configuration as Bi(III).[14] They all point toward the central lacuna where the $[BiI_6]^{3-}$ unit will be subsequently inserted. These ELF basins are quite diffuse (V = 12.6 $Å^3$) and populated by 1.17 electrons. Upon assembling of the fragments, these basins do not vanish and the Bi−(μ_3-I_c) bonds formed remain significantly longer than those in the $[Bi_6I_{18}]$ crown. However, we observe a strong contraction of these ELF basins with a volume reduced to 5.0 $Å^3$ with a population of 0.80 e. Upon insertion of the $[BiI_6]^{3-}$ unit, the Bi_6 planar ring of the $[Bi_6I_{18}]$ crown adapts to diminish the electronic repulsion between the

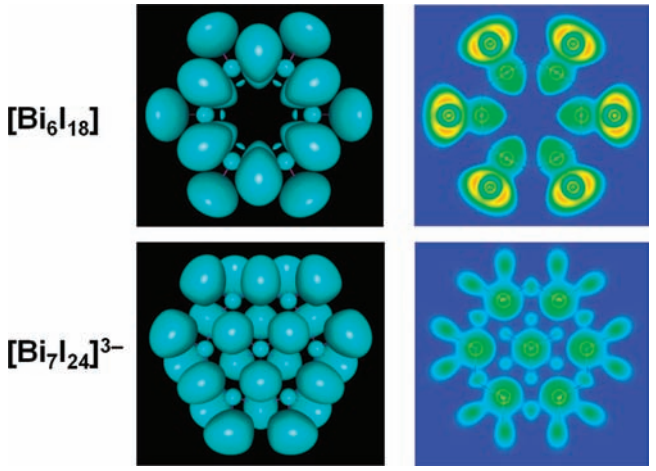

Figure 4. Top view into the ELF surfaces of $[Bi_6I_{18}]$ and $[Bi_7I_{24}]^{3-}$ (left) and their ELF contours (right) (η^{iso} plot is 0.5).

iodines of the central octahedral fragment and the bismuth crown valence basins. This leads to expansion of the $[Bi_6I_{18}]$ crown. By comparison between the ELF functions with and without dispersion correction along a $Bi_{crown}-Bi_{center}$ axis (Figure S4, Supporting Information), we find that addition of a dispersion term results in a smaller crown dilatation because it counterbalances the repulsion between the electrons valence basins. As a result, the ELF basins are more diffuse when dispersion is introduced. In addition, the absence of $Bi_{crown}-Bi_{crown}$ ELF valence basins is indicative of the absence of electron delocalization within the planar Bi_6 hexagon. Furthermore, the crown is isolated from the central $[BiI_6]^{3-}$ fragment by the presence of the bismuth crown ELF basins. The computed ELF surface of $[Bi_7I_{24}]^{3-}$ favors model A over B.

The validity of model A is further supported on the energy level. Although both association processes A and B, illustrated in Figure 3, are energetically favorable, the energy required to form the kinetically stable, gas-phase $[Bi_7I_{24}]^{3-}$ structure is lower in the case of model A, $\Delta E_1^{BP86\text{-}D}$ = −219 kcal mol^{-1} compared to $\Delta E_2^{BP86\text{-}D}$ = −1456 kcal mol^{-1} in model B, owing to the energetically high-lying fragments in the latter case.

The molecular orbital (MO) scheme of $[Bi_7I_{24}]^{3-}$ also favors bonding model A. The molecular orbital diagrams of the trianion and its fragments are characterized by a set of alternating metal−ligand 'bands' typical for common POM

dx.doi.org/10.1021/ic201859c | Inorg. Chem. 2012, 51, 1562−1568

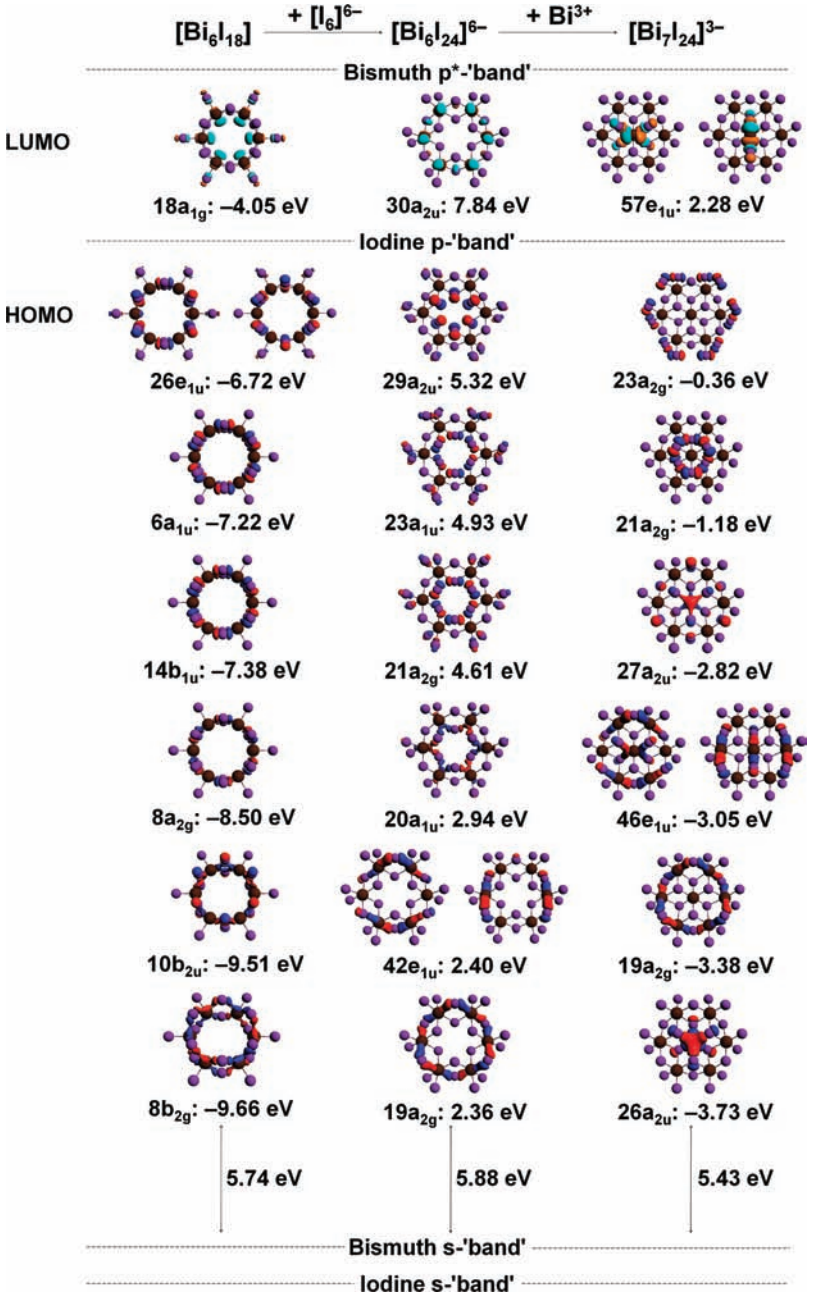

Figure 5. Spatial representation of the most relevant molecular orbitals of $[Bi_6I_{18}]$ (left), $[Bi_6I_{24}]^{6-}$ (center), and $[Bi_7I_{24}]^{3-}$ (right) (±0.03 isosurface value) obtained from the ZORA-BP86-D/TZ2P computations in the gas phase.

structures[5b,f] (Figure 5). The lowest unoccupied level (LUMO) of $[Bi_7I_{24}]^{3-}$ is the unfilled p*-metal $57e_{1u}$ orbital with ca. 60% contribution from Bi (bismuth 'band'), whereas the highest occupied molecular orbital (HOMO), $23a_{2g}$, and the large set of lower-lying HOMOs correspond to levels of *a* and *e* symmetry which characterize participation of the iodine (I_t, I_b, I_c) $p_{x,y,z}$ orbitals (iodine 'band'). The energy gap spanned by this valence p 'band' is ca. 11 eV.

The low-lying MOs ($27a_{2u}$, $19a_{2g}$, $26a_{2u}$) of the iodine 'band' deserve special attention. The $27a_{2u}$ and $26a_{2u}$ MOs correspond to the central $[BiI_6]^{3-}$ fragment inside the $[Bi_6I_{18}]$ crown. These MOs, showing orbital delocalization above and below the central bismuth atom, arise because of noncovalent I···I interactions ($d_{I\cdots I}$ = 439.8−450.1 pm), which result in multicenter E···E···E 3c2e bonding (E = I; WBI = 0). The latter is promoted by the p orbitals of the central bismuth atom. The $19a_{2g}$ MO shows the delocalized σ bonding of p−p orbital character along the interpenetrating Bi−I_b closed loops (puckered $\{Bi_6I_6\}$ ring). Interestingly, the interpenetrating metal−oxygen closed loops form the macrocyclic bonding[1S] present in most POM structures.[5] For instance, the Anderson-type POM anions of the type $[TeM_6O_{24}]^{6-}$ (M = Mo, W) display metal−oxygen closed loops of σ(d)- and π(d)-orbital character.[5b] The MO diagrams of the $[Bi_6I_{24}]^{6-}$ and $[Bi_6I_{18}]$ crowns are characterized by the presence of similar interpenetrating closed loops, $19a_{2g}$ and $8b_{2g}$, respectively (Figure 5). In addition, we note that analysis of the iodobismuthate anions showed that their molecular orbitals in the gas phase lie much higher in energy than those obtained from the computations in a condensed medium, i.e., in thf solution.

dx.doi.org/10.1021/ic201859c | *Inorg. Chem.* 2012, 51, 1562−1568

Table 1. Energy Decomposition Analysis (kcal mol^{-1}) of the Interactions between $[BiI_6]^{3-}$ and $[Bi_6I_{18}]$ within I

functional	ΔE_{int} [a]	ΔE_{Pauli}	ΔV_{elstat}	ΔE_{oi}	ΔE_{disp}	ΔE_{def} [b]	D_e [c]
BP86	−232.4	259.8	−275.2	−217.0		56.0	176.4
BP86-D	−286.3	341.7	−322.5	−243.5	−62.0	66.8	219.5

[a] $\Delta E_{int} = \Delta V_{elstat} + \Delta E_{Pauli} + \Delta E_{oi} + \Delta E_{disp}$ (see Figure 3). [b] Deformation (or preparation) energy, ΔE_{def} (see Figure 3). [c] $\Delta E = -D_e = \Delta E_{int} + \Delta E_{def}$.

The gap ($\Delta E_{HOMO-LUMO}$) between the valence (filled) and the unfilled band of $[Bi_7I_{24}]^{3-}$ is 2.65 eV. According to their band gap values (3.76 and 3.33 eV, respectively), the Anderson-type $[Bi_7X_{24}]^{3-}$ (X = Cl, Br) structures are even kinetically more stable than $[Bi_7I_{24}]^{3-}$. The latter should thus have a higher reactivity and is moreover the most dispersion-dependent framework within the $[Bi_7X_{24}]^{3-}$ series (Table S5, Supporting Information). The contribution of the dispersion energy, ΔE_{disp}, to the total bonding energy, ΔE_{total}, of $[Bi_7X_{24}]^{3-}$ increases in the order X = Cl (2.9%) < Br (4.3%) < I (7.0%).

In order to gain deeper insight into $[Bi_7I_{24}]^{3-}$ and related iodobismuthate anions, we carried out DFT calculations on the known, high-nuclearity extended structures $[Bi_5I_{19}]^{4-}$,[16] $[Bi_6I_{22}]^{4-}$,[16,17] and $[Bi_8I_{28}]^{4-}$[18] from the $[Bi_nI_{3n+m}]^{4-}$ family and $[Bi_8I_{30}]^{6-}$[19] from the $[Bi_nI_{3n+m}]^{6-}$ family (Tables S1 and S5, Supporting Information). The kinetic stability of these anions is slightly lower than that of $[Bi_7I_{24}]^{3-}$, and it moderately decreases with increasing nuclearity of the anionic framework. The contribution of ΔE_{disp} to ΔE_{total} for these anions is slightly lower than that observed for $[Bi_7I_{24}]^{3-}$ (7.0%), and it increases in the order $[Bi_5I_{19}]^{4-}$ (6.1%) < $[Bi_8I_{30}]^{6-}$ (6.4%) ≤ $[Bi_6I_{22}]^{4-}$ (6.4%) < $[Bi_8I_{28}]^{4-}$ (6.9%).

To take into account the macroscopic solvent (thf) effects, the dispersion-corrected BP86-D functional was combined with the conductor-like screening model (COSMO) of solvation with the solvent-excluding surface (SES).[20] The results obtained for $[Bi_7I_{24}]^{3-}$ indicate that the condensed medium has an effect mainly on the Bi···Bi distances. These are reduced by ca. 1.5% in solution (Figure S3 and Table S5, Supporting Information). Such a reduction of the Bi···Bi distances is observed for $[Bi_7X_{24}]^{3-}$ with X = Cl (1.7%), Br (1.6%), and I (1.5%). In the case of $[Bi_5I_{19}]^{4-}$, $[Bi_6I_{22}]^{4-}$, $[Bi_8I_{28}]^{4-}$, and $[Bi_8I_{30}]$,$^{4-}$ their Bi···Bi distances are reduced by 2−10% in thf. While the kinetic stability of the $[Bi_7X_{24}]^{3-}$ anions in solution increases only smoothly (by less than 0.05 eV), the difference in the kinetic stability of $[Bi_5I_{19}]^{4-}$, $[Bi_6I_{22}]^{4-}$, $[Bi_8I_{28}]^{4-}$, and $[Bi_8I_{30}]^{6-}$ between the gas phase and solution is even larger (in the range of ca. 0.1−0.4 eV). The contribution of ΔE_{disp} to ΔE_{total} for the anionic frameworks $[Bi_7X_{24}]^{3-}$, $[Bi_5I_{19}]^{4-}$, $[Bi_6I_{22}]^{4-}$, $[Bi_8I_{28}]^{4-}$, and $[Bi_8I_{30}]^{6-}$, of which the structures were optimized in solution, decreases compared to the gas phase (Table S5, Supporting Information). From inspection of the contributions of solvation energy, ΔE_{solv}, to ΔE_{total} for $[Bi_7X_{24}]^{3-}$, $[Bi_5I_{19}]^{4-}$, $[Bi_6I_{22}]^{4-}$, $[Bi_8I_{28}]^{4-}$, and $[Bi_8I_{30}]^{6-}$ it should be stated the following: (i) the contribution of ΔE_{solv} to ΔE_{total} for $[Bi_7X_{24}]^{3-}$ increases when going down the group 17 halogens in the order of X = Cl (6.9%) < Br (7.3%) < I (7.8%); (ii) the contribution of ΔE_{solv} to ΔE_{total} for the four-charged anionic $[Bi_5I_{19}]^{4-}$ (18.1%), $[Bi_6I_{22}]^{4-}$ (14.9%), and $[Bi_8I_{28}]^{4-}$ (10.8%) decreases with increasing nuclearity of the iodobismuthate within the $[Bi_nI_{3n+m}]^{m-}$ family; and (iii) the contribution of ΔE_{solv} to ΔE_{total} (21% for $[Bi_8I_{30}]^{6-}$) rises with increasing the net negative charge of the iodobismuthate anion.

The energy decomposition analysis (EDA) for the framework **I** is given in Table 1 (see also Table S6, Supporting Information). The EDA for the interaction between $[BiI_6]^{3-}$ and $[Bi_6I_{18}]$ within the trianion **I** indicates that the nature of the ion−cage interaction is predominantly electrostatic (ΔV_{elstat} is around 56% of the bonding interactions, i.e., $\Delta V_{elstat} + \Delta E_{oi}$), albeit the orbital interaction term, ΔE_{oi} (ca. 44%), also significantly contributes to the attractive interaction between the fragments $[BiI_6]^{3-}$ and $[Bi_6I_{18}]$. Analysis of this ΔE_{oi} term shows that the interpenetrating Bi−I closed loops (likewise the M−O ones in the POMs)[5a,b] do not contribute much to the bonding stability of **I**. While the orbital interaction in the A_{2g} symmetry group is only ca. −17 kcal mol^{-1}, the largest orbital interactions in **I** are in the E_{1u} and E_{1g} groups (around −80 kcal mol^{-1}). The attractive or stabilizing effects ($\Delta V_{elstat} + \Delta E_{disp}$) in **I** overall outweigh the substantial contribution from the Pauli repulsion term, ΔE_{Pauli}, which is liable for the destabilization of the orbital-interaction effects ($\Delta E_{orb} + \Delta E_{Pauli}$)[21] within **I**. The preparation or deformation energy (denoted as ΔE_{def}) of **I**, which is the energy difference between the equilibrium structures of $[BiI_6]^{3-}$ and $[Bi_6I_{18}]$ and the energy of these fragments in the geometry that they acquire in the trianionic structure **I**, is relatively high. The major deformation takes place mainly in the $[Bi_6I_{18}]$ moiety surrounding the $[BiI_6]^{3-}$ subunit. The calculated values of the dissociation energies D_e for **I** reveal that the internal interactions are very strong (Figure 3 and Table 1). The results from the EDA of **I** are in line with the EDA calculations reported by Bridgeman and Cavigliasso in their work on the Anderson-type heteropolyanions of the type $[TeM_6O_{24}]^{6-}$ (M = Mo, W),[5b] where the stabilizing interactions between $[TeO_6]^{3-}$ and the neutral $[M_6O_{18}]$ fragment within the $[TeM_6O_{24}]^{6-}$ framework originate from two relative contributions, ΔV_{elstat} and ΔE_{oi}, of 66% and 34%, respectively.

CONCLUSIONS

The very sensitive compound **1**·4H_2O has been obtained by a ligand-exchange reaction between $[Pd(OAc)_2]$ and BiI_3 under ambient conditions. The known oxophilicity of bismuth is the likely driving force for formation and structural arrangement of **1**·4H_2O, which was established by X-ray diffraction. Furthermore, by including water molecules in the cavities of the molecular assembly illustrated in Figure 2, **1**·4H_2O displays a behavior similar to that of polyoxometalates[4,5] and their analogues[11] since in their crystals the presence of water molecules is well established. $[Bi_7I_{24}]^{3-}$ is the largest iodobismuthate anion observed for trianionic species and is the first heptanuclear framework in the family of iodobismuthates. This newly established structure constitutes a new member of a larger family of iodobismuthates of general formula $[Bi_nI_{3n+m}]^{m-}$ which may be predicted to exist (see Table S1, Supporting Information).

The London dispersion forces play a crucial role in the self-organization of the anionic structural motive of **1**·4H_2O, namely, the heptanuclear $[Bi_7I_{24}]^{3-}$. Their origin is the repulsive interaction between the crown bismuth valence basins and those of the iodines of the central $[BiI_6]^{3-}$ unit. Such interactions should be less relevant in the POMs (e.g.,

dx.doi.org/10.1021/ic201859c | Inorg. Chem. 2012, 51, 1562−1568

polyoxomolybdates and polyoxotungstates) because in their case the active orbitals are more contracted, partially filled 4d or 5d orbitals. These should be compared to the bismuth more diffuse and polarizable 6p orbitals, populated by charge transfer from the iodines. The structural arrangement of the main group Anderson-type $[Bi_7I_{24}]^{3-}$ anion can be understood in terms of the "ion-cage" model (A), which is the most relevant one and finds a parallel in the model elaborated for the Anderson-type POMs. Thus, the kinetic stabilization of the $[BiI_6]^{3-}$ unit within **I** has its origin in the attractive contributions from both orbital and electrostatic terms, charge transfer, as well as dispersion forces. Unique interpenetrating metal−ligand closed loops observed in $[Bi_7I_{24}]^{3-}$ are the "fingerprint" of the analogy between the main group and the transition metal Anderson-type structures. As observed in many POMs, the overall kinetic stability of the cation−anion architecture is associated with the solvent molecules attached to the countercations of the complex anion. Such experimental findings and theoretical analyses provide excellent opportunities to build further bridges between main group and transition metal chemistry.

■ ASSOCIATED CONTENT

Supporting Information

Stoichiometry matrix for the iodobismuthate ions, synthesis and structural date of **1**·4H_2O (CCDC 855004). Computational details including geometrical, electronic and energetic parameters of the complexes $[Bi_7X_{24}]^{3-}$ (X = Cl, Br, I), of the fragments constitutive of $[Bi_7I_{24}]^{3-}$, and of the high-nuclearity extended structures $[Bi_5I_{19}]^{4-}$, $[Bi_6I_{22}]^{4-}$, $[Bi_8I_{28}]^{4-}$, and $[Bi_8I_{30}]^{6-}$. This material is available free of charge via the Internet at http://pubs.acs.org.

■ AUTHOR INFORMATION

Corresponding Author

* E-mail: braunstein@unistra.fr.

■ ACKNOWLEDGMENTS

The authors are grateful to the Deutsche Forschungsgemeinschaft (DFG) for a postdoctoral fellowship to K.Y.M., the CNRS, the Ministère de l'Enseignement Supérieur et de la Recherche (Paris), and the Université de Strasbourg for support. They also thank le Centre d'Etudes du Calcul Parallèle et de la Visualisation (CECPV) for allocation of computer resources and time.

■ DEDICATION

§Dedicted to Hubert Le Bozec on the occasion of his 60th birthday.

■ REFERENCES

(1) Hoffmann, R. *Angew. Chem., Int. Ed.* **1982**, *21*, 711.

(2) (a) Braunstein, P.; Raithby, P. R.; Oro, L. A. *Metal Clusters in Chemistry*; Wiley-VCH: Weinheim, 1999; Vol. 3, p 1798. (b) Braunstein, P.; Rosé, J. In *Comprehensive Organometallic Chemistry*, 2nd ed.; Abel, E. W., Stone, F. G. A., Wilkinson, G., Eds.; Pergamon Press: Oxford, 1995; Vol. *10*, Chapter 7, pp 351−385. (c) Braunstein, P.; Rosé, J. In *Catalysis by Di- and Polynuclear Metal Clusters*; Adams, R. D., Cotton, F. A., Eds.; John Wiley: New York, 1998; pp 443−508. (d) Braunstein, P.; Rosé, J. In *Catalysis in Metal Clusters in Chemistry*; Braunstein, P., Oro, L. A., Raithby, P. R., Eds.; Wiley-VCH: Weinheim, Germany, 1999; Vol. 2, pp 616−677.

(3) (a) Driess, M. *Acc. Chem. Res.* **1999**, *32*, 1017. (b) Driess, M. *Pure Appl. Chem.* **1999**, *71*, 437. (c) Linti, G.; Köstler, W.; Pritzkow, H. *Eur. J. Inorg. Chem.* **2002**, 2643. (d) Monakhov, K. Yu.; Linti, G.; Wolters, L. P.; Bickelhaupt, F. M. *Inorg. Chem.* **2011**, *50*, 5755.

(4) (a) Berzelius, J. J. *Poggendorf's Ann. Phys. Chem.* **1826**, *6*, 369. (b) In *Heteropoly and Isopoly Oxometalates*; Pope, M. T., Ed.; Springer-Verlag: Berlin, 1983. (c) Kozhevnikov, I. *Chem. Rev.* **1998**, *98*, 171. (d) Mizuno, N.; Misono, M. *Chem. Rev.* **1998**, *98*, 199. (e) Coronado, E.; Gómez-García, C. J. *Chem. Rev.* **1998**, *98*, 273. (f) Rhule, J. T.; Hill, C. H.; Judd, D. A.; Schinazi, R. *Chem. Rev.* **1998**, *98*, 327. (g) Tsuji, H.; Koyasu, Y. *J. Am. Chem. Soc.* **2002**, *124*, 5608. (h) Dolbecq, A.; Dumas, E.; Mayer, C. R.; Mialane, P. *Chem. Rev.* **2010**, *110*, 6009. (i) Putaj, P.; Lefebvre, F. *Coord. Chem. Rev.* **2011**, *255*, 1642.

(5) For the theoretical works, see, for example: (a) Bridgeman, A.; Cavigliasso, G. *Inorg. Chem.* **2002**, *41*, 1761. (b) Bridgeman, A.; Cavigliasso, G. *J. Phys. Chem. A* **2003**, *107*, 6613. (c) Bridgeman, A. *Chem.—Eur. J.* **2006**, *12*, 2094. (d) Fernandez, J. A.; López, X.; Bo, C.; de Graaf, C.; Baerends, E. J.; Poblet, J. M. *J. Am. Chem. Soc.* **2007**, *129*, 12244. (e) Rodríguez-Fortea, A.; Vilà-Nadal, L.; Poblet, J. M. *Inorg. Chem.* **2008**, *47*, 7745. (f) Romo, S.; Antonova, N. S.; Carbó, J. J.; Poblet, J. M. *Dalton Trans.* **2008**, 5166. (g) Romo, S.; de Graaf, C.; Poblet, J. M. *Chem. Phys. Lett.* **2008**, *450*, 391. (h) Vilà-Nadal, L.; Rodríguez-Fortea, A.; Yan, L.; Wilson, E.; Cronin, L.; Poblet, J. M. *Angew. Chem., Int. Ed.* **2009**, *48*, 5452.

(6) See, for example: (a) Louvain, N.; Mercier, N.; Boucher, F. *Inorg. Chem.* **2009**, *48*, 879. (b) Chen, Y.; Yang, Z.; Guo, C.-X.; Ni, C.-Y.; Ren, Z.-G.; Li, H.-X; Lang, J.-P. *Eur. J. Inorg. Chem.* **2010**, 5326. (c) Goforth, A. M.; Tershansy, M. A.; Smith, M. D.; Peterson, L. Jr.; Kelley, J. G.; DeBenedetti, W. J. I.; zur Loye, H.-C. *J. Am. Chem. Soc.* **2011**, *133*, 603.

(7) (a) Fisher, G. A.; Norman, N. C. *Adv. Inorg. Chem.* **1994**, *41*, 233. (b) Wu, L.-M.; Wu, X.-T.; Chen, L. *Coord. Chem. Rev.* **2009**, *253*, 2787. References cited therein.

(8) Carmalt, C. J.; Clegg, W.; Elsegood, M. R. J.; Errington, R. J.; Havelock, J.; Lightfoot, P.; Norman, N. C.; Scott, A. J. *Inorg. Chem.* **1996**, *35*, 3709. In this work, the authors reported the complex $[Na_3(thf)_x][Bi_7I_{24}]$ which is extremely sensitive to loss of thf. The compound was obtained when BiI_3 was crystallized from thf/hexanes mixtures. Observation of sodium in the reported compound is associated with the presence of some NaI in the sample of BiI_3.

(9) Crystal data for **1**·4H_2O: $3(C_{20}H_{38}BiO_8)$,Bi_7I_{24},4(O), M = 6418.91 g mol^{-1}, T = 173(2) K, trigonal, space group $R\bar{3}c$, a [Å] = 27.2955(7), b [Å] = 27.2955(7), c [Å] = 31.6049(13), γ [°] = 120, V [Å^3] = 20392.3(11), Z = 6, D_{calcd} [g cm^{-3}] = 3.136, μ [mm^{-1}] = 18.395, R_1 [$I > 2\sigma(I)$] = 0.0615 (2395 observed), wR_2 (all data) = 0.2155 for 4210 data (4091 independent), 96 parameters, and 27 restraints. Goodness of fit (S) on F^2 1.142. Max/min 3.479/−3.564 e Å^{-3}. Two oxygen atoms, corresponding to two molecules of water, were located on special positions with occupancy factors of 1/6 and 1/2, most likely corresponding to four oxygen atoms of water molecules per unit of complex **1**, considering the space group multiplicity. Their hydrogen atoms could not be located and refined. They were thus omitted in the model formula. CCDC 855004.

(10) (a) Holleman, F. A.; Wiberg, N. *Lehrbuch der Anorganischen Chemie*, 34th ed.; Walter de Gruyter: Berlin, 1995, 1838. (b) Silvestru, C.; Breunig, H. J.; Althaus, H. *Chem. Rev.* **1999**, *99*, 3277. (c) Mantina, M.; Chamberlin, A. C.; Valero, R.; Cramer, C. J.; Truhlar, D. G. *J. Phys. Chem. A* **2009**, *113*, 5806.

(11) (a) Zhang, J.; Teo, P.; Pattacini, R.; Kermagoret, A.; Welter, R.; Rogez, G.; Hor, T. S. A.; Braunstein, P. *Angew. Chem., Int. Ed.* **2010**, *49*, 4443. (b) Pattacini, R.; Teo, P.; Zhang, J.; Lan, Y.; Powell, A. K.; Nehrkorn, J.; Waldmann, O.; Hor, T. S. A.; Braunstein, P. *Dalton Trans.* **2011**, *40*, 10526.

(12) (a) Grimme, S. *J. Comput. Chem.* **2006**, *27*, 1787. (b) Grimme, S.; Anthony, J.; Ehrlich, S.; Krieg, H. *J. Chem. Phys.* **2010**, *132*, 154104.

(13) Grimme, S.; Huenerbein, R.; Ehrlich, S. *ChemPhysChem* **2011**, *12*, 1258.

(14) van Severen, M.-C.; Gourlaouen, C.; Parisel, O. *J. Comput. Chem.* **2010**, *31*, 185.

(15) (a) Nomiya, K.; Miwa, M. *Polyhedron* **1985**, *4*, 89. (b) Nomiya, K.; Miwa, M. *Polyhedron* **1985**, *4*, 675. (c) Nomiya, K.; Miwa, M. *Polyhedron* **1985**, *4*, 1407. (d) Nomiya, K. *Polyhedron* **1987**, *6*, 309.
(16) Krautscheid, H. *Z. Anorg. Allg. Chem.* **1994**, *620*, 1559.
(17) (a) Clegg, W.; Errington, R. J.; Fisher, G. A.; Green, M. E.; Hockless, D. C. R.; Norman, N. C. *Chem. Ber.* **1991**, *124*, 2457. (b) Eickmeier, H.; Jaschinski, B.; Hepp, A.; Nuss, J.; Reuter, H.; Blachnik, R. *Z. Naturforsch., B: Chem. Sci.* **1999**, *54*, 305. (c) Goforth, A. M.; Peterson, L. Jr.; Smith, M. D.; zur Loye, H.-C. *J. Solid State Chem.* **2005**, *178*, 3529. (d) Liu, B.; Xu, L.; Guo, G.-C.; Huang, J.-S. *J. Solid State Chem.* **2006**, *179*, 1611. (e) Tershansy, M. A.; Goforth, A. M.; Smith, M. D.; Peterson, L. Jr.; zur Loye, H.-C. *Acta Crystallogr., Sect. E: Struct. Rep. Online* **2006**, *62*, m3269.
(18) (a) Krautscheid, H. *Z. Anorg. Allg. Chem.* **1995**, *621*, 2049. (b) Sharutin, V. V.; Egorova, I. V.; Klepikov, N. N.; Boyarkina, T. A.; Sharutina, O. K. *Zh. Neorg. Khim. (Russ. J. Inorg. Chem.)* **2009**, *54*, 1768.
(19) Feldmann, C. *J. Solid State Chem.* **2003**, *172*, 53.
(20) (a) Klamt, A.; Schüürmann, G. *J. Chem. Soc., Perkin Trans.* **1993**, *2*, 799. (b) Klamt, A. *J. Phys. Chem.* **1995**, *99*, 2224. (c) Klamt, A.; Jones, V. *J. Chem. Phys.* **1996**, *105*, 9972.
(21) Krapp, A.; Bickelhaupt, F. M.; Frenking, G. *Chem. Eur. J.* **2006**, *12*, 9196.